



Improved fault quantification for a plate structure

Sanghyun Choi^a, Sooyong Park^{b,*}, Nam-Hoi Park^c, Norris Stubbs^d

^a*Department of Railroad Facility Engineering, Korea National Railroad College, 374-18 Wolam-dong, Uiwang-si, Kyounggi-do 437-763, Republic of Korea*

^b*Division of Architecture and Ocean Space, Korea Maritime University, Dongsam-dong, Pusan 606-791, Republic of Korea*

^c*Korea Institute of Construction and Transportation Technology Evaluation and Planning, 1600 Kwanyang-dong, Antang 431-060, Republic of Korea*

^d*Department of Civil Engineering, Texas A&M University, College Station, TX 77843, USA*

Received 25 January 2006; received in revised form 10 April 2006; accepted 2 May 2006

Available online 22 June 2006

Abstract

In this paper, an improved damage quantification methodology for a plate structure is presented. The methodology utilizes the relationship between the stiffness loss and the fractional changes of the modal parameters due to damage. To improve the damage quantification performance, the methodology is derived by eliminating erroneous assumptions in the existing modeshape-based methods and adopting additional modal information, i.e., natural frequencies. The basic elements of the approach are summarized in this paper, and the validity of the proposed method is demonstrated using numerical data from a simply-supported plate structure. In the numerical verification, the damage quantification performance of the proposed method is compared with the performance of other existing methods. Also, the effects of incomplete measurement and noisy modal test data on the accuracy of damage quantification are discussed. The result shows the proposed method yields superior damage quantification results to the existing algorithms.

© 2006 Elsevier Ltd. All rights reserved.

1. Introduction

During the past few decades, there have been intense interests and activities to research and develop technologies for health monitoring and diagnostics of civil structures such as buildings and bridges [1]. Health maintenance and operation of aging structures depend largely on the ability to assess conditions of the structure via nondestructively detecting and evaluating damage in the structures. Currently available nondestructive damage detection (NDD) techniques include visual inspection, nondestructive testing (NDT), and vibration-based damage evaluation methods.

The visual inspection method is probably the most common approach in inspecting a structure. However, the method is only effective in finding damage on the surface of the structure and limited to an accessible area. The NDT techniques include acoustic or ultrasonic methods, magnetic field methods, radiographs, eddy-current methods, and thermal field methods [2]. These methods can provide accurate and detailed information

*Corresponding author. Tel.: +82 51 410 4588; fax: +82 51 403 8841.

E-mail addresses: schoi86@nate.com (S. Choi), sypark@bada.hhu.ac.kr (S. Park), nhpark@kictep.re.kr (N.H. Park), n-stubbs@tamu.edu (N. Stubbs).

Nomenclature			
		F	fraction of modal strain energy
		k	flexural rigidity of the plate
*	superscript for parameters for the damaged structure	k_j	flexural rigidity of the element j in the plate
α_j	severity of damage for j th element	K	system stiffness matrix
α_i^p	predicted severity of damage for i th element	K_i	i th modal stiffness matrix
α_i^t	true severity of damage for i th element	M	system mass matrix
β_j	damage index for element j	M_i	i th modal mass matrix
ρ	density	NDE	number of damaged elements
ϕ_i	i th modeshape vector	NE	number of elements
ϕ_j	j th modeshape vector with noise	NM	number of modes
ν	Poisson's ratio	NSE	number of surrounding elements
μ_β, σ_β	mean and the standard deviation of β_j 's	s	flexural compliance of the plate
η	level of significance of the test	s_j	flexural compliance of the element j in the plate
λ	eigenvalue	t	thickness of the plate
A	area of the plate	U	modal strain energy
A_j	area of the element j in the plate	z_j	standardized damage index for the j th element
e	percentage of random noise	z_η	threshold value
E	modulus of elasticity		

for a specific portion of a structure. However, these techniques require that the vicinity of the damage be known a priori, and that the portion of the structure being inspected be readily accessible. In addition, most NDT methods can only detect potential damage on or near the surface of the structure.

Another approach for NDD comprises vibration-based methods that attempt to detect damage and simultaneously assess the condition of a structure using the dynamic response of the structure. The basic idea behind these vibration-based methods is that changes in the physical properties of a structural system alter the dynamic response characteristics of the structure (i.e., frequencies, damping, and modeshapes). These methods have recently received much attention as the need for developing an effective and practical structural health monitoring system emerges as a prominent research issue in structural engineering. To date, numerous vibration-based NDD methods have been presented as a result of worldwide research efforts [3,4].

Even though many approaches have been presented and published in the field of NDD, only a few applications on detecting and identifying damage in plate-type structures have been published. The first attempt was made by Cawley and Adams [5]. They introduced a method to locate the defects in a plate structure using frequency information. However, frequency information only has been known to be not enough for identifying damage in a large structure due to their insensitivity to small damage [6]. Chen and Swamidass [7] presented numerical results for a cantilever plate containing a crack by comparing strain modeshapes. Chance et al. [8] presented damage detection results for a cantilever plate. In their study, they showed that the curvature of the modeshapes was more likely to locate the damage than modeshapes. These two studies, however, failed to provide a practical procedure for localizing and quantifying damage in a plate structure. Choi and Stubbs [9] proposed two NDD algorithms for a plate structure—one from the governing differential equation of motion (the compliance method) and the other from the expression for the elastic strain energy of a plate (the strain energy method). However, the compliance method included the fourth-order numerical differentiation which introduced additional numerical error, and the strain energy method, which is the simple extension of the damage index method [10], showed poor damage quantification performance [11]. Experimental verification of the application of the damage index method to a plate structure was provided by Cornwell et al. [12]. Araujo dos Santos et al. [13] proposed a damage quantification method using the changes in eigenvalues and modeshapes. However, their method is not practical for a real structure because it requires a significant number of frequencies and corresponding modeshapes to yield reliable

solutions, which is not usually measurable from real structures. Li and Yam [14] introduced a damage localization method using the changes in modal sensitivities. Also, Wu and Law [15] proposed a damage localization method using uniform load surface curvature. Later, they proposed a sensitivity-based model updating approach incorporating uniform load surface curvatures to identify the severity of damage in a plate structure [16,17]. Other researchers proposed NDD methods that can locate and quantify damage in a plate structure, recently. Lee and Shin [18] developed an iterative procedure that can locate and size damage. Also, Choi et al. [19] proposed a modal-compliance-based damage quantification method which can relieve the difficulty in numerical differentiation of the compliance method [9].

Despite these research efforts, however, the following problems related to vibration-based NDD methods still remain unsolved to date. First, significant number of modal information is required to yield reliable solutions [13]. Second, only damage localization scheme is provided [14,15]. Third, significant amount of computational work is needed to identify damage information [16–18]. Fourth, poor damage quantification results are obtained for identified damage locations [9,11].

The objective of this paper is to present a simple but robust NDD methodology that can improve the performance of damage quantification for a plate structure. In order to achieve the stated objective, the following tasks are performed. First, the existing NDD algorithms based on the modal strain energy change [11] and the modal compliance change [19] are outlined and reviewed. Then, a new NDD algorithm to improve the performance of damage quantification is formulated based on the relationship between the stiffness loss and the fractional changes of the modal parameters, i.e., modeshapes and natural frequencies, in which erratic assumptions of the existing NDD algorithms [11,19] are eliminated. Finally, the performance of each algorithm is evaluated by comparing the accuracy of damage prediction results via a numerical example of a simply-supported plate structure. In the example, possible problems such as the effect of noise and incomplete measurement when applied to real structures are also addressed. The effect of measurement noise on damage identification is investigated by applying random noise to modeshape data.

2. Theory

2.1. Strain energy index

The damage index method developed by Stubbs et al. [10] utilizes the change in the modal strain energy distribution in a structure due to damage. The extension of the damage index method to a plate structure [9–11] can be stated as follows.

Considering a thin and undamaged plate structure, the modal strain energy for the i th mode, U_i , is given by [20]

$$U_i = \frac{1}{2} \int \int_A k \left\{ (\kappa_{xx,i} + \kappa_{yy,i})^2 - 2(1 - \nu) [\kappa_{xx,i}\kappa_{yy,i} - \kappa_{xy,i}^2] \right\} dA, \quad (1)$$

where

$$\kappa_{xx,i} = \frac{\partial^2 \phi_i}{\partial x^2}, \quad \kappa_{yy,i} = \frac{\partial^2 \phi_i}{\partial y^2}, \quad \kappa_{xy,i} = \frac{\partial^2 \phi_i}{\partial x \partial y} \quad \text{and} \quad k = \frac{Et^3}{12(1 - \nu^2)}. \quad (2)$$

Assuming the flexural rigidity, k , is constant in an element of the structure, the modal strain energy for the i th mode that is concentrated in the j th element is given by

$$U_{ij} = \frac{1}{2} k_j \int \int_{A_j} \left\{ (\kappa_{xx,i} + \kappa_{yy,i})^2 - 2(1 - \nu) [\kappa_{xx,i}\kappa_{yy,i} - \kappa_{xy,i}^2] \right\} dA = k_j \gamma_{ij}, \quad (3)$$

where

$$\gamma_{ij} = \frac{1}{2} \int \int_{A_j} \left\{ (\kappa_{xx,i} + \kappa_{yy,i})^2 - 2(1 - \nu) (\kappa_{xx,i}\kappa_{yy,i} - \kappa_{xy,i}^2) \right\} dA. \quad (4)$$

Note that the term γ_{ij} involves only geometric quantities and Poisson's ratio. Eq. (4) can be rewritten for the damaged structure

$$U_{ij}^* = k_j^* \gamma_{ij}^*. \quad (5)$$

The fraction of modal strain energy for the i th mode that is concentrated in the j th member (i.e., the element sensitivity of the j th member to the i th mode) is given by

$$F_{ij} = U_{ij}/U_i. \quad (6)$$

The change in the fraction of modal energy of the j th member in the i th mode can be expressed as

$$dF_{ij} = F_{ij}^* - F_{ij} = \frac{U_{ij}}{U_i} \left[\frac{dU_{ij}}{U_i} - \frac{dU_i}{U_i} \right], \quad (7)$$

where the superscript asterisks represent the parameters for the damaged structure. Assuming that the structure is damaged at a single location j ($dU_i/U_i \approx 0$) and that the modal force is constant while k_j changes, the quantity dF_j can be obtained from the first-order expansion [21]

$$dF_{ij} \approx -F_{ij} \alpha_j, \quad (8)$$

where the fractional change in stiffness, α_j , is given by

$$\alpha_j = \frac{dk_j}{k_j} = \frac{k_j^* - k_j}{k_j}. \quad (9)$$

Define a damage index for the j th element as $\beta_j = k_j/k_j^*$. Then substituting Eqs. (3), (5), (6), (8) and (9) into Eq. (7) and simplifying yield the damage index for the element j as follows

$$\beta_j = \frac{k_j}{k_j^*} \approx \frac{1}{2} \left[\frac{\gamma_{ij}^*/\sum_{j=1}^{NE} \gamma_{ij}^* + 1}{\gamma_{ij}/\sum_{j=1}^{NE} \gamma_{ij} + 1} + 1 \right]. \quad (10)$$

For NM eigenmodes, the composite form of the damage index is defined as

$$\beta_j = \frac{k_j}{k_j^*} \approx \frac{1}{2} \left[\frac{\sum_{i=1}^{NM} \left(\gamma_{ij}^*/\sum_{j=1}^{NM} \gamma_{ij}^* \right) + 1}{\sum_{i=1}^{NM} \left(\gamma_{ij}/\sum_{j=1}^{NM} \gamma_{ij} \right) + 1} + 1 \right]. \quad (11)$$

Note that, in the damage index in Eqs. (10) and (11), the domain of interest in the problem is shifted by adding unity to the denominator and numerator to avoid numerical errors when both numerator and denominator are close to zero. Note also that in general improved damage estimation results can be obtained by utilizing the composite form of the damage index when multiple modes are available [9,11,19,22]. The damage indices in Eqs. (10) and (11) will be referred as the strain energy index throughout the remainder of this paper. More detailed derivation of Eqs. (10) and (11) can be found in Ref. [11].

2.2. Modal compliance index

The modal compliance method utilizes the changes in the distribution of the modal compliance of a structure due to damage [22]. The extension of the modal compliance method to a plate structure was presented by Choi et al. [19]. The modal-compliance-based damage index for the plate structure derived from the invariance relationship between the bending moments and the curvatures is presented as

$$\beta_{ij}^c = \frac{s_j^*}{s_j} \approx \frac{\int_{\Delta} \int_{A_j} (\kappa_{xx,i}^* + \kappa_{yy,i}^*) dA + 1}{\int_{\Delta} \int_{A_j} (\kappa_{xx,i} + \kappa_{yy,i}) dA + 1}. \quad (12)$$

Note that Eq. (12) is derived based on the assumption that the modal force is constant while s_j changes. For NM eigenmodes, the composite form of the damage index is defined as

$$\beta_{ij}^c = \frac{s_j^*}{s_j} \approx \frac{\sum_{i=1}^{NM} \int_{\Delta} \int_{A_j} (\kappa_{xx,i}^* + \kappa_{yy,i}^*) dA + 1}{\sum_{i=1}^{NM} \int_{\Delta} \int_{A_j} (\kappa_{xx,i} + \kappa_{yy,i}) dA + 1}. \tag{13}$$

Detailed derivation of Eqs. (12) and (13) can be found in Ref. [19]. Note that in Eqs. (12) and (13), the domain of both numerator and denominator are shifted by adding unity to avoid numerical errors. Note also that the damage indices in Eqs. (12) and (13) will be referred as the compliance index throughout the remainder of this paper.

2.3. New damage index

The effectiveness of the damage indices presented in Eqs. (11) and (13) were verified using numerical [11] and experimental data [12,19]. However, while the algorithms were successful in identifying damage locations, they consistently produced lower damage severity estimations [11]. In this section, a new NDD methodology is developed by eliminating erratic assumptions in the existing NDD algorithms. Errors can be included in the existing NDD algorithms, since values of the damage index obtained from Eqs. (11) and (13) are based on the following assumption (s): (1) it is assumed that the modal force is constant while k_j changes; and (2) the second term is neglected in Eq. (7) with the condition that $U_i \gg U_{ij}$.

Here, a new algorithm that can possibly improve the performance of damage estimation is presented by eliminating erratic assumptions and including additional modal information, i.e., resonant frequencies. The new damage index can be derived as follows.

Consider the following eigenvalue problem associated with a plate system

$$(K - \lambda M)\phi = 0. \tag{14}$$

For the plate system of n degree-of-freedoms, Eq. (14) yields n equations of the form

$$\lambda_i = K_i/M_i = \phi_i^T K \phi_i / \phi_i^T M \phi_i. \tag{15}$$

Taking the first-order approximation of Eq. (15) and simplifying yields

$$\frac{d\lambda_i}{\lambda_i} = \frac{dK_i}{K_i} - \frac{dM_i}{M_i}. \tag{16}$$

Assuming the change in mass is negligible, Eq. (16) can be reduced to

$$\frac{d\lambda_i}{\lambda_i} = \frac{dK_i}{K_i}. \tag{17}$$

Eq. (17) can be rewritten in terms of modal strain energy as

$$\frac{d\lambda_i}{\lambda_i} = \frac{dU_i}{U_i} \tag{18}$$

or

$$\frac{\lambda_i^*}{\lambda_i} = \frac{U_i^*}{U_i}. \tag{19}$$

Substituting Eqs. (3) and (5) into Eq. (19) and simplifying yield

$$\beta_{ij} = \frac{k_j}{k_j^*} = \frac{\lambda_i \gamma_{ij}^*}{\lambda_i^* \gamma_{ij}}. \tag{20}$$

Shifting the axis of reference for the sensitivities from $\lambda_i^* \gamma_{ij} = 0$ and $\lambda_i \gamma_{ij}^* = 0$ to $\lambda_i^* \gamma_{ij} = -1$ and $\lambda_i \gamma_{ij}^* = -1$, respectively, to overcome the division-by-zero difficulty yields the non-singular function, β_{ij} :

$$\beta_{ij} = \frac{k_j}{k_j^*} = \frac{\lambda_i \gamma_{ij}^* + 1}{\lambda_i^* \gamma_{ij} + 1}. \tag{21}$$

Note that the terms, γ_{ij} and γ_{ij}^* , in Eq. (21) can be determined from a knowledge of the geometry of the structure and measurable pre- and post-damage modeshapes (ϕ_i and ϕ_i^*). For each element j , there are as many β_{ij} 's available as there are modeshapes. The following expression is the composite form of damage index β_j for a single location when NM modes are available

$$\beta_j = \frac{\sum_{i=1}^{NM} \lambda_i \gamma_{ij}^* + 1}{\sum_{i=1}^{NM} \lambda_i^* \gamma_{ij} + 1} \tag{22}$$

Note that in deriving the damage index expressions in Eqs. (20)–(22), the stated assumptions involved in the existing strain energy and compliance indices are not utilized.

2.4. Damage localization and severity estimation

Next, we establish the criteria for damage localization based on statistical reasoning. The values, $\beta_1, \beta_2, \beta_3, \dots, \beta_{NE}$ for each element, are considered as realization of a random variable. The standardized damage indicator, z_j , is given by

$$z_j = \frac{\beta_j - \mu_\beta}{\sigma_\beta}. \tag{23}$$

The final step in damage localization is classification. Classification analysis addresses itself to the problem of assigning an object to one of a number of possible groups on the basis of observations made on the objects. There are two groups: undamaged elements and damaged elements. The observations made on the objects are the β_j 's. Many techniques are available to accomplish the classification of objects. In this paper, the method of classification utilizes the Neyman–Pearson criteria [23]. Let H_0 be the hypothesis that structure is not damaged at the element j , and let H_1 be the hypothesis that structure is damaged at the element j . The following decision rules may be used to assign damage to the element j : (a) choose H_0 if $z_j < z_\eta$ and (b) choose H_1 if $z_j \geq z_\eta$ where η is a threshold which assigns a confidence level for the presence of damage.

The damage severities may be obtained using the corresponding non-standardized damage indices (e.g., Eq. (20)). However, since the damage index for an element is estimated using the response measures, which are determined based on the properties of joining elements, the effect of damage spreads out to surrounding elements, which is called the smear effect in this paper. As a result, much smaller severity has been obtained for the damaged element [11]. To overcome this difficulty, the severity of damage for a possible damaged element is obtained by summing the severity indices for the damaged element and the surrounding elements. Thus, the

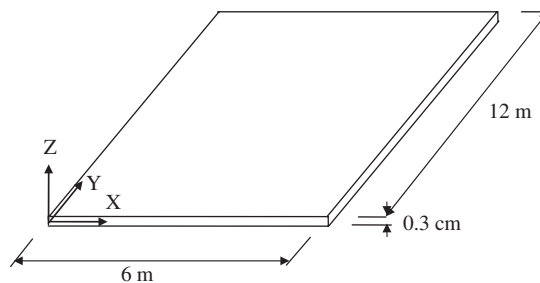


Fig. 1. Schematic of the example structure.

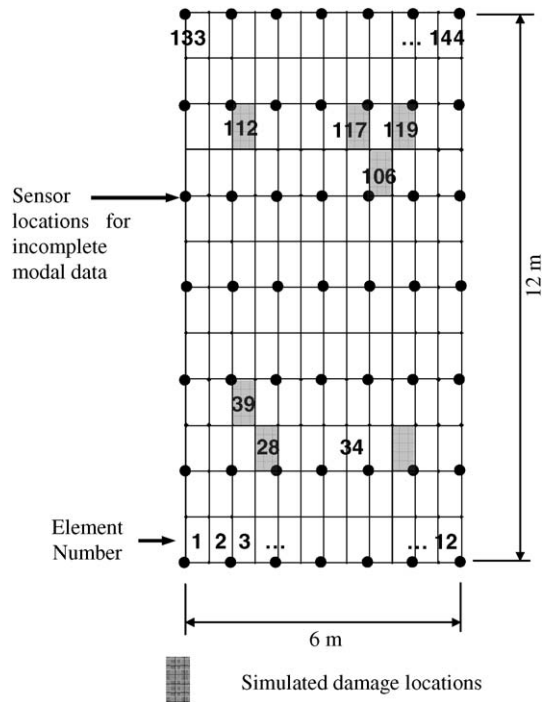


Fig. 2. Simulated damage locations.

Table 1
Simulated damage locations and severities

Damage scenario	Elements damaged	Corresponding severity (%)
1	28	10
2	119	10
3	34	10
4	112	30
5	34, 106	10, 10
6	39, 117	30, 20

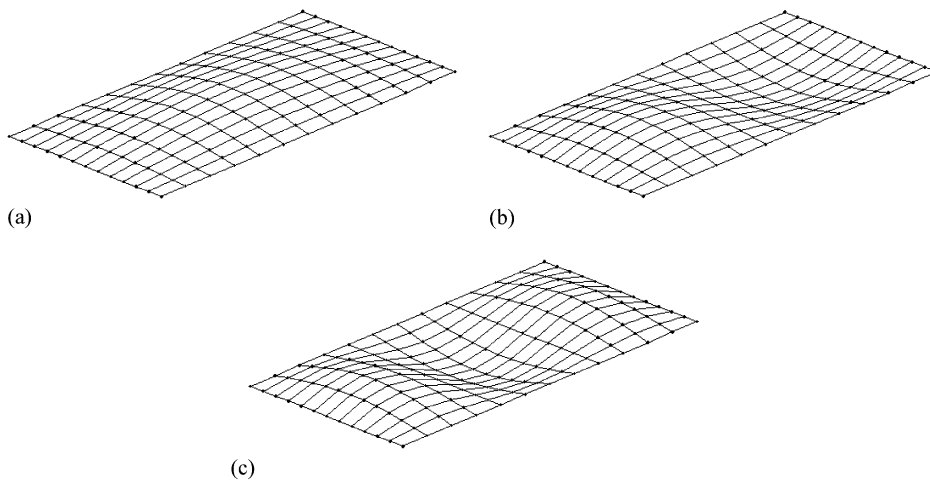


Fig. 3. Modeshapes of the example plate: (a) mode 1 (7.78 Hz), (b) mode 2 (12.54 Hz), (c) mode 3 (21.05 Hz).

severity of damage for j th element may be expressed as

$$\alpha_j = \alpha_j + \sum_{m=1}^{NSE} \alpha_m = (1/\beta_j - 1) + \sum_{m=1}^{NSE} (1/\beta_m - 1). \quad (24)$$

Note that the severity (magnitude) of damage obtained using Eq. (24) represents the fractional stiffness loss for a specific element j of the structure. Note also that Eq. (24) is only valid when surrounding elements have no damage.

Table 2
Natural frequencies of the example plate

Damage scenario	Mode 1 (Hz)	Mode 2 (Hz)	Mode 3 (Hz)
Undamaged	7.782	12.537	21.046
1	7.779	12.530	21.034
2	7.780	12.535	21.042
3	7.779	12.532	21.039
4	7.773	12.514	21.008
5	7.777	12.528	21.033
6	7.767	12.508	21.002

Table 3
Percentage of false negative error (%)

Case	Noise-free			1% noise			3% noise			Incomplete measurements		
	A ^a	B ^b	C ^c	A	B	C	A	B	C	A	B	C
1	0	0	0	0	0	0	0	0	0	0	0	0
2	0	0	0	0	0	0	0	0	0	0	0	0
3	0	0	0	0	0	0	0	0	0	0	0	0
4	0	0	0	0	0	0	0	0	0	0	0	0
5	0	0	0	0	0	0	0	0	0	0	0	0
6	0	0	0	0	0	0	50	0	0	0	0	0
Avg.	0	0	0	0	0	0	13	0	0	0	0	0

^aDamage identification results using the strain energy index method.

^bDamage identification results using the compliance index method.

^cDamage identification results using the new method.

Table 4
Percentage of false positive error

Case	Noise-free			1% noise			3% noise			Incomplete measurements		
	A ^a	B ^b	C ^c	A	B	C	A	B	C	A	B	C
1	4.9	3.5	4.2	5.6	3.5	4.2	6.3	5.6	5.6	4.9	8.4	8.4
2	7.0	3.5	4.9	7.0	4.2	4.9	7.3	7.0	6.3	5.6	8.4	6.3
3	5.6	3.5	4.9	6.3	4.9	4.9	6.3	6.3	6.3	5.6	7.0	6.3
4	4.9	3.5	4.2	4.9	3.5	4.9	5.6	5.6	6.3	4.9	8.4	8.4
5	5.6	6.3	7.0	5.6	7.0	7.0	6.3	7.0	7.0	4.9	6.3	8.4
6	4.9	6.3	4.2	4.9	7.0	5.6	5.6	7.0	7.0	4.9	8.4	9.1
Avg.	5.5	4.4	4.9	5.7	5.0	5.3	6.2	6.4	6.4	5.1	7.8	7.8

^aDamage identification results using the strain energy index method.

^bDamage identification results using the compliance index method.

^cDamage identification results using the new method.

Table 5
Severity estimation results

Case	True size (%)	Noise-free			1% noise			3% noise			Incomplete measurements		
		A (mse)	B	C	A	B	C	A	B	C	A	B	C
1	10	6.2 (0.38)	6.5 (0.35)	9.4 (0.06)	6.0 (0.40)	6.1 (0.39)	9.2 (0.08)	3.9 (0.61)	4.5 (0.55)	8.5 (0.15)	3.5 (0.65)	4.2 (0.58)	7.4 (0.26)
2	10	6.7 (0.33)	7.9 (0.21)	10.4 (0.04)	6.5 (0.35)	7.6 (0.24)	10.0 (0.00)	6.0 (0.40)	5.8 (0.42)	9.2 (0.08)	2.1 (0.79)	3.1 (0.69)	5.6 (0.44)
3	10	6.2 (0.38)	6.7 (0.33)	9.9 (0.01)	5.8 (0.42)	6.1 (0.39)	9.9 (0.01)	4.8 (0.52)	5.3 (0.47)	8.7 (0.13)	3.8 (0.62)	4.4 (0.56)	8.0 (0.20)
4	30	21.3 (0.29)	21.7 (0.28)	31.4 (0.05)	20.3 (0.32)	19.8 (0.34)	29.8 (0.01)	15.5 (0.48)	16.8 (0.44)	24.8 (0.17)	12.5 (0.58)	14.0 (0.53)	24.8 (0.17)
5	10	5.7 (0.44)	6.7 (0.39)	10.1 (0.05)	5.5 (0.48)	6.2 (0.44)	9.6 (0.07)	4.6 (0.58)	3.6 (0.66)	7.3 (0.25)	3.4 (0.73)	4.1 (0.71)	8.0 (0.43)
6	10	5.6 (0.44)	5.5 (0.39)	9.2 (0.05)	5.0 (0.48)	5.1 (0.44)	9.0 (0.07)	3.8 (0.58)	3.2 (0.66)	7.8 (0.25)	2.1 (0.73)	1.8 (0.71)	3.4 (0.43)
6	20	11.3 (0.39)	12.2 (0.40)	19.6 (0.02)	10.6 (0.43)	11.6 (0.43)	19.0 (0.05)	– (0.77)	8.9 (0.53)	17.6 (0.14)	6.5 (0.71)	6.4 (0.71)	10.7 (0.47)
6	30	19.5 (0.39)	17.8 (0.40)	29.7 (0.02)	18.3 (0.43)	16.8 (0.43)	28.4 (0.05)	13.6 (0.77)	14.9 (0.53)	25.3 (0.14)	7.7 (0.71)	7.6 (0.71)	16.0 (0.47)
Avg. mse		0.37	0.33	0.04	0.40	0.37	0.04	0.56	0.51	0.15	0.68	0.63	0.33

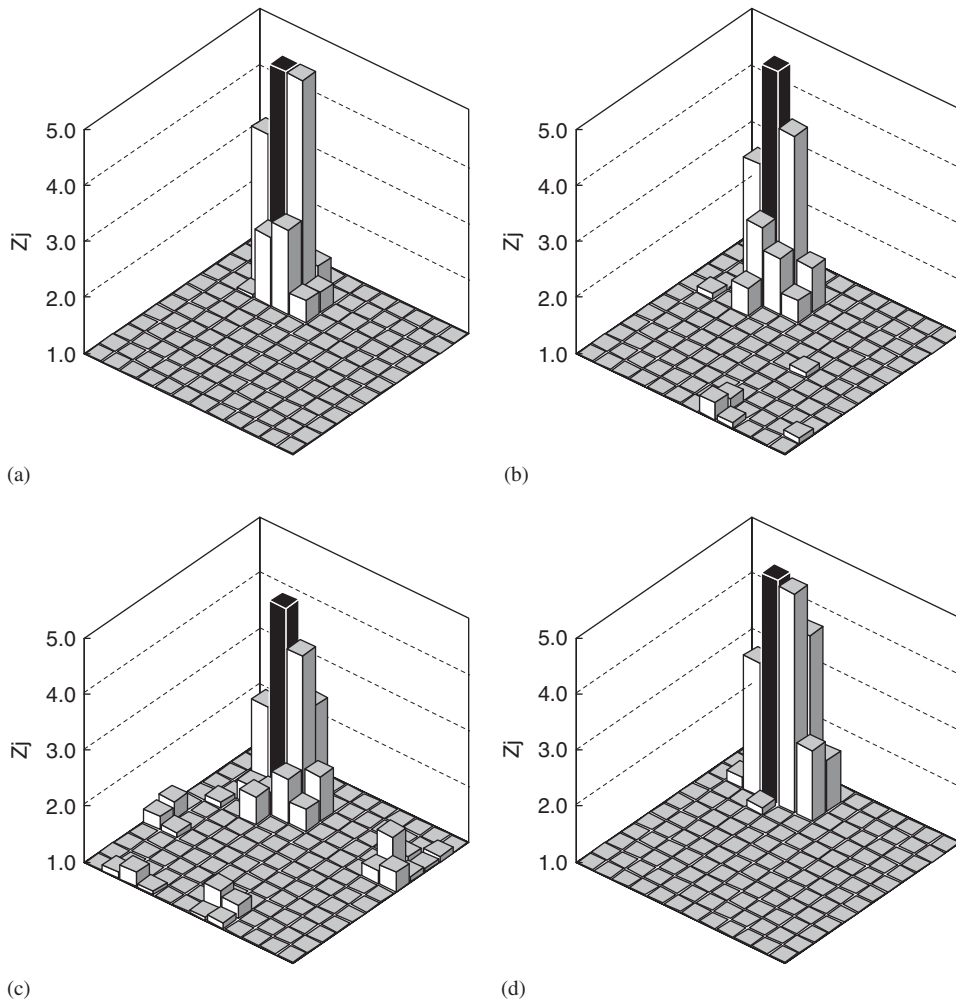


Fig. 4. Damage localization results for damage case 1 using the strain energy index method: (a) 0% noise, (b) 1% noise, (c) 3% noise, and (d) incomplete measurement.

3. Numerical verification

The feasibility and the performance of the proposed NDD algorithm are examined via a numerical example of an all-edge simply supported plate structure. The size of plate is $6\text{ m} \times 12\text{ m}$ as shown in Fig. 1. Four-node plate elements are used to model the example structure. The model has 144 elements (12×12) and 169 nodes and the size of each element is $0.5\text{ m} \times 1.0\text{ m}$ (Fig. 2). All elements are assumed to be made of the same material with $E = 25\text{ GPa}$, $\rho = 2400\text{ kg/m}^3$, $\nu = 0.15$, and $t = 15\text{ cm}$. The structure is subjected to six damage scenarios. Simulated damage ranges from one to two locations and corresponding severities range from 10% to 30%. Table 1 lists the element number and corresponding magnitude of the inflicted damage for each scenario. To simulate the damage, the elastic modulus of the element corresponding to the location of the damage is reduced. A free vibration analysis is performed using ABAQUS[®] [24]. The first three bending modeshapes and natural frequencies of the plate structure utilized in the damage identification are shown in Fig. 3 and Table 2, respectively.

Using the damage indices, the localization and size of potential damage in the structure is implemented using the following steps. First, the damage index for each element is calculated using Eqs. (11), (13), and (22) for each damage algorithm. Second, the obtained damage indices are standardized using Eq. (23). Third, the presence of damage in element j is determined according to the pre-assigned classification rules: (a) the element

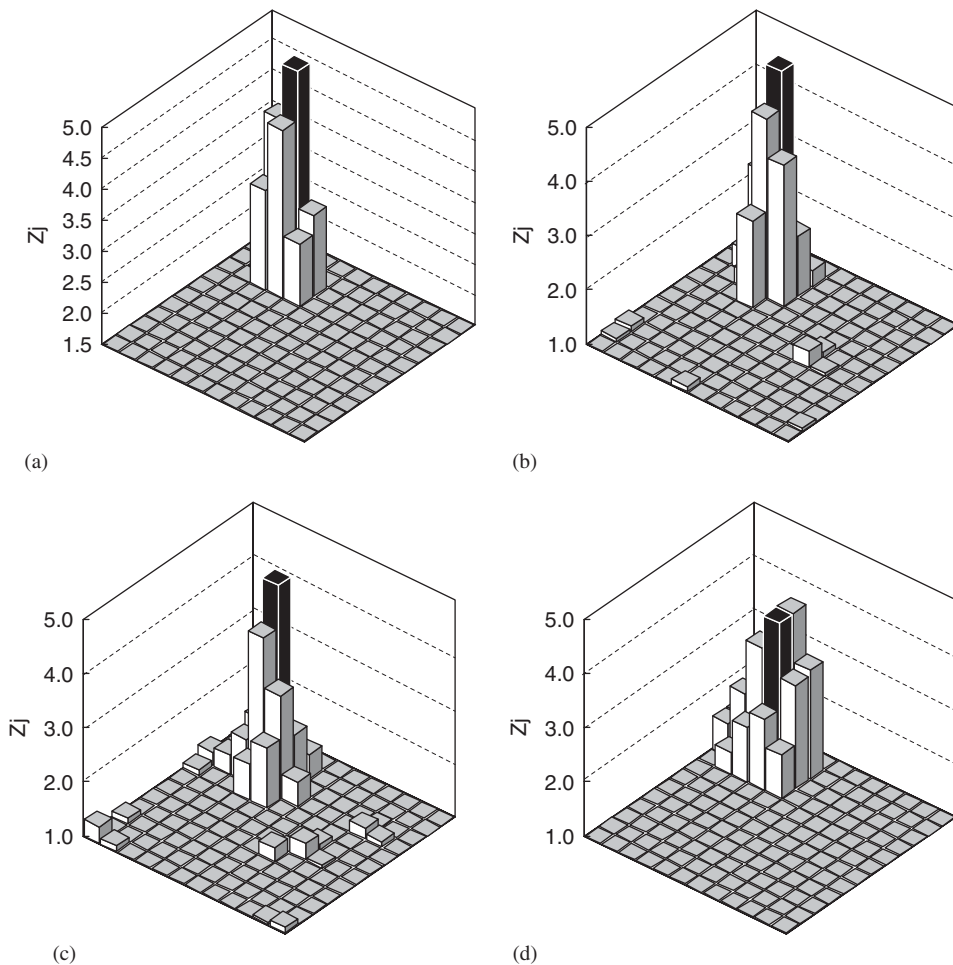


Fig. 5. Damage localization results for damage case 1 using the compliance index method: (a) 0% noise, (b) 1% noise, (c) 3% noise, and (d) incomplete measurement.

is damaged if $z_j \geq 1.5$; (b) the element is not damaged if $z_j < 1.5$. Note that the value of damage threshold, 1.5, corresponds to 93% confidence level for the presence of damage. Finally, the severity of damage for each classified location is estimated using Eq. (24). Note that, for every single predicted damage location, the severity of damage is estimated by adding the calculated severities of the surrounding elements to the estimated severity of the element itself. For instance, in damage case 1, the damage severity of element 28 is estimated by summing the calculated α_s for elements 15, 16, 17, 27, 28, 29, 39, 40, and 41.

To verify the field applicability of the proposed method, the damage evaluation with incomplete and noisy data is conducted. Firstly, the effect of noise is simulated by adding a series of random noise generated from a uniform distribution on the interval $[-1, 1]$ to the original modeshapes of the structure. An $e\%$ random noise is added to the modal displacement vector as follows:

$$\tilde{\phi}_j = \phi_j \left(1 + \frac{e}{100} \times \text{random noise} \right). \quad (25)$$

In present applications, the effect of different level of noise on damage identification is investigated by applying 1% and 3% random noise. Secondly, the effect of the incomplete modal data is simulated by performing damage identification using modal data from only 49 locations as depicted in Fig. 2.

The accuracy of the damage prediction can be quantified by such criteria as: the percentage of false positives, the percentage of false negatives, and mean sizing error. A false positive means that damage is

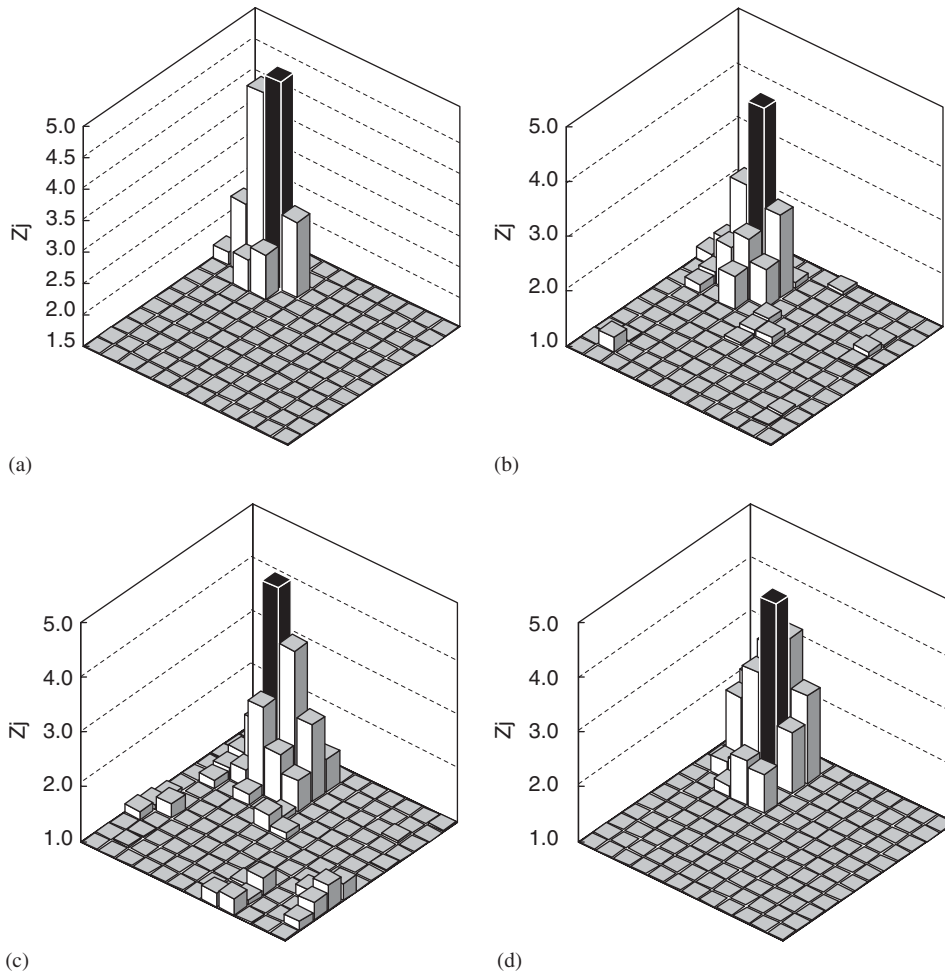


Fig. 6. Damage localization results for damage case 1 using the new method: (a) 0% noise, (b) 1% noise, (c) 3% noise, and (d) incomplete measurement.

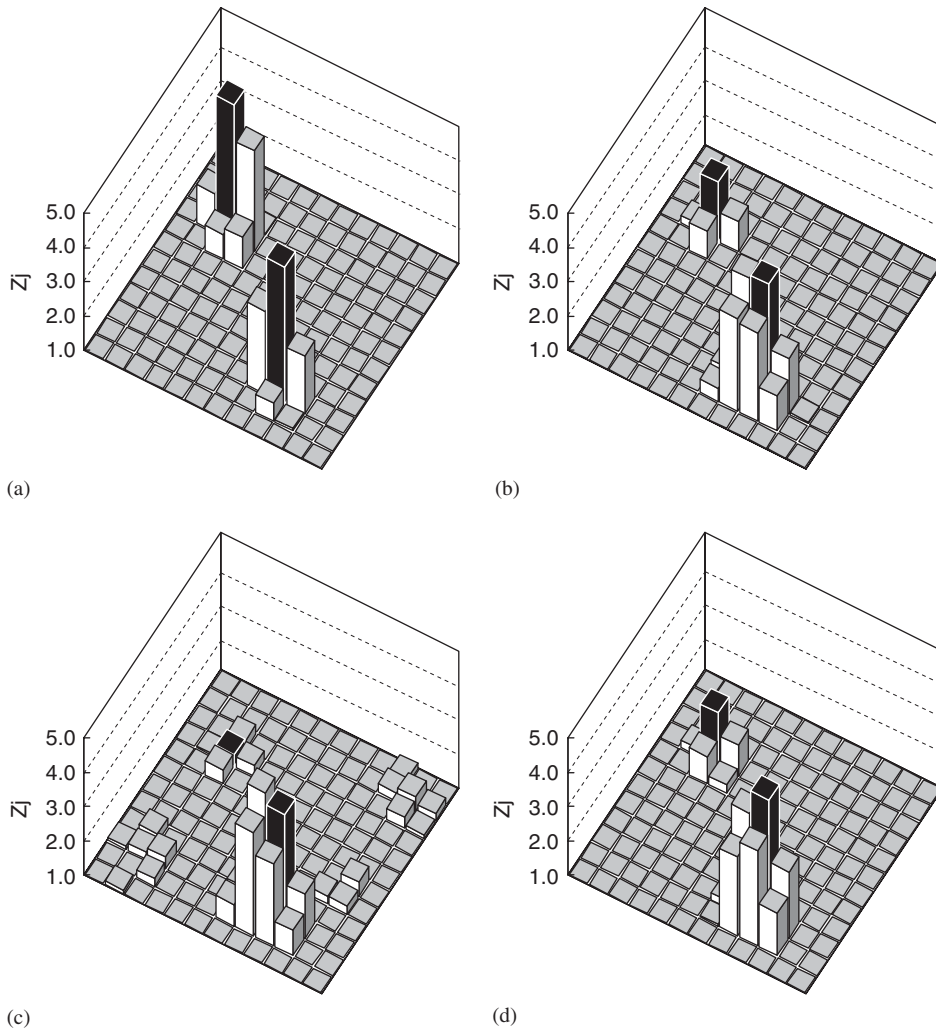


Fig. 7. Damage localization results for damage case 6 using the strain energy index method: (a) 0% noise, (b) 1% noise, (c) 3% noise, and (d) incomplete measurement.

reported where no damage exists and a false negative means that damage is not reported where damage exists. The percentage of false positive error is calculated by dividing the number of false positive predictions by the number of undamaged elements, and the percentage of false negative error is calculated by dividing the number of false negative predictions by the number of damaged elements. The false positive and the false negative may reflect the quality of the measured data and the effectiveness of damage localization algorithm. Note that, in an ideal situation, the false positive and the false negative error rates should be zero. As a measure of damage quantification error, mean sizing error (mse) is selected that is defined as [25]

$$\text{mse} = \frac{1}{NDE} \sum_{i=1}^{NDE} \left| \frac{\alpha_i^t - \alpha_i^p}{\alpha_i^t} \right|. \quad (26)$$

The damage identification results are summarized in Tables 3–5. The resulting percentage of false negatives and false positives for each damage case are summarized in Tables 3 and 4, respectively. In Table 3, it can be seen that the three algorithms identified all damages successfully except one case—damage case 6 using the

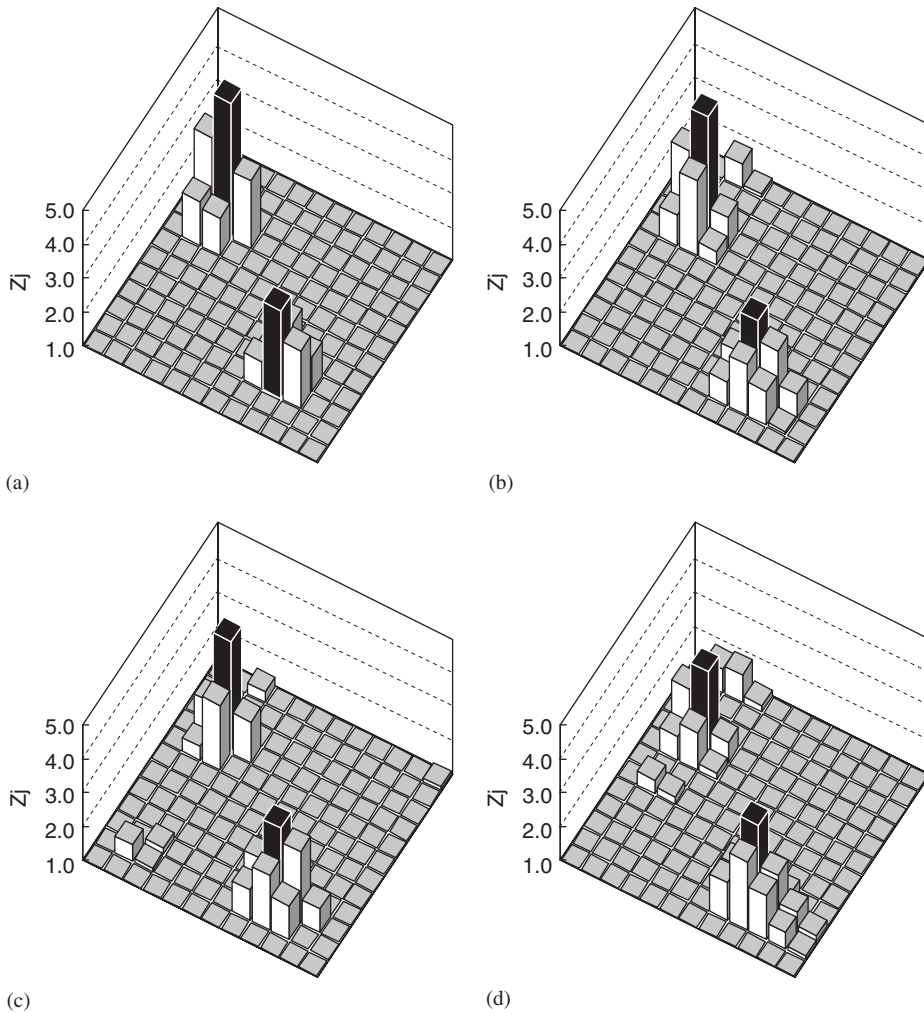


Fig. 8. Damage localization results for damage case 6 using the compliance index method: (a) 0% noise, (b) 1% noise, (c) 3% noise, and (d) incomplete measurement.

strain energy index algorithm when 3% noise is applied. In Table 4, it is observed that the false identification error was increased when the incomplete modal data were utilized. However, the error percentage seems not to be influenced significantly by increasing the number of damage locations and the noise level. The severity estimation results are listed in Table 5. In the table, it is observed that the proposed algorithm yield superior quantification results to the other two existing algorithms. The table also shows that the noise affects the accuracy of the damage quantification. As expected, the quantification error is increasing as the noise level increases. However, it is observed that the accuracy of the estimated severities is more decreased with incomplete modal data than with noise-polluted data up to a 3% noise level.

The damage localization results are visualized in Figs. 4–9. Note that only the damage localization results for damage cases 1 and 6 are presented due to space limitation. The obtained standardized damage index for each element is presented in those figures. In the figures, the elements corresponding to the inflicted locations of damage are in black color. As seen in the figures, most false damage predictions arise in the vicinity of the simulated damage locations. When random noise is introduced, the effect of noise is almost negligible up to the 3% noise level, which corroborates the robustness of the presented methodology. The effect of incomplete sensor locations also can be seen in the figures. Due to the numerical interpolation between the assumed sensor locations, the effect of damage is more smeared into the neighboring elements.

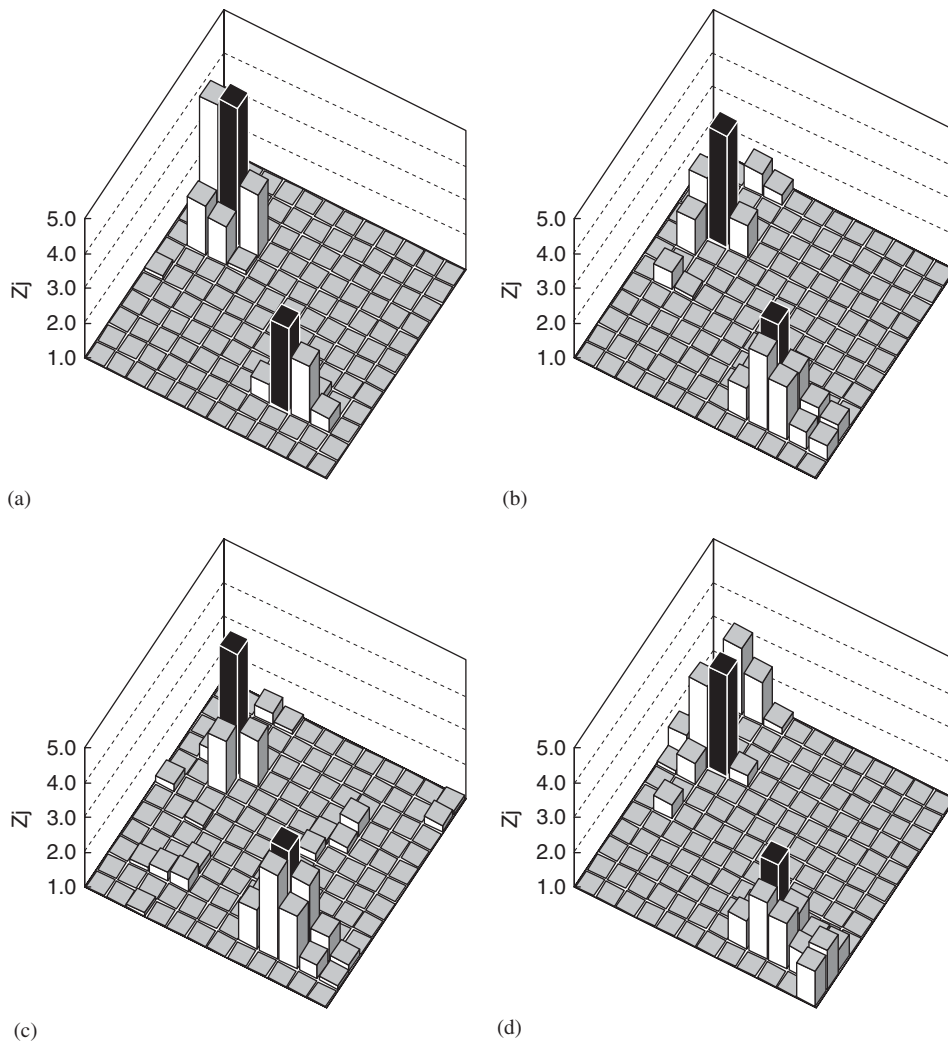


Fig. 9. Damage localization results for damage case 6 using the new method: (a) 0% noise, (b) 1% noise, (c) 3% noise, and (d) incomplete measurement.

4. Conclusions

In this paper, a new NDD method that can improve the performance of damage quantification was presented. The methodology utilizes the relationship between the stiffness loss and the changes in the natural frequencies and the modeshapes of a structure. The validity of the methodology was demonstrated using numerical data from a simply-supported plate structure. From the study, the following conclusions are drawn:

1. the proposed methodology based on the change in the element-level modal strain energies and the natural frequencies can be used for damage localization and severity estimation for plate structures;
2. the numerical study using a simply-supported plate structure reveals that the proposed methodology can identify single and multiple damage locations with noisy and incomplete data;
3. the proposed methodology can yield superior damage quantification results to the existing damage index and compliance index algorithms; and
4. the accuracy of the estimated severity using the proposed methodology is more decreased with incomplete modal data than with noise-polluted data up to 3% noise level.

References

- [1] C. Farrar, D. Jauregui, Damage detection algorithms applied to experimental and numerical modal data from the I-40 bridge, Technical Report LA-13074-MS, Los Alamos National Laboratory, 1996.
- [2] D.R. Askeland, *The Science and Engineering of Materials*, PWS Publishing Company, Boston, 1994.
- [3] S.W. Doebling, C. Farrar, M.B. Prime, D.W. Shevitz, Damage identification and health monitoring of structural and mechanical systems from changes in their vibrational characteristics: a literature review, Technical Report LA-13070-MS, Los Alamos National Laboratory, 1996.
- [4] Y. Zou, L. Tong, G.P. Steven, Vibration-based model-dependent damage (delamination) identification and health monitoring for composite structures, *Journal of Sound and Vibration* 230 (2) (2000) 357–378.
- [5] P. Cawley, R.D. Adams, The location of defects in structures from measurements of natural frequencies, *Journal of Strain Analysis* 14 (2) (1979) 49–57.
- [6] A.K. Pandey, M. Biswas, Damage detection in structures using changes in flexibility, *Journal of Sound and Vibration* 169 (1) (1994) 3–17.
- [7] Y. Chen, A.S.J. Swamidias, Dynamic characteristics and modal parameters of a plate with a small growing surface crack, *Proceedings of the 12th International Modal Analysis Conference* (1994) 1155–1161.
- [8] J. Chance, G.R. Tomlinson, K. Worden, A simplified approach to the numerical and experimental modeling of the dynamics of a cracked beam, *Proceedings of the 12th International Modal Analysis Conference* (1994) 778–785.
- [9] S. Choi, N. Stubbs, Nondestructive damage detection algorithms for 2D plates, *SPIE Proceedings: Smart Structures and Materials* 3043 (1997) 193–204.
- [10] N. Stubbs, S. Park, C. Sikorsky, S. Choi, A global nondestructive damage assessment methodology for civil engineering structures, *International Journal of Systems Science* 31 (11) (2000) 1361–1373.
- [11] S. Choi, Development of nondestructive damage detection algorithms for plate structures, *KSCE Journal of Civil Engineering* 6 (4) (2002) 495–501.
- [12] P. Cornwell, S.W. Doebling, C.R. Farrar, Application of the strain energy damage detection method to plate-like structures, *Journal of Sound and Vibration* 224 (2) (1999) 359–374.
- [13] J.V. Araujo dos Santos, C.M. Mota Soares, C.A. Mota Soares, H.L.G. Pina, Development of a numerical model for the damage identification on composite plate structures, *Composite Structures* 48 (2000) 59–65.
- [14] Y.Y. Li, L.H. Yam, Sensitivity analysis of sensor locations for vibration control and damage detection of thin-plate systems, *Journal of Sound and Vibration* 240 (4) (2001) 623–636.
- [15] D. Wu, S.S. Law, Damage localization in plate structures from uniform load surface curvature, *Journal of Sound and Vibration* 276 (1–2) (2004) 227–244.
- [16] D. Wu, S.S. Law, Anisotropic damage model for an inclined crack in thick plate and sensitivity study for its detection, *International Journal of Solids and Structures* 41 (2004) 4321–4336.
- [17] D. Wu, S.S. Law, Sensitivity of uniform load surface curvature for damage identification in plate structures, *Journal of Vibration and Acoustics* 127 (2) (2005) 84–92.
- [18] U. Lee, J. Shin, A structural damage identification method for plate structures, *Engineering Structures* 24 (2002) 1177–1188.
- [19] S. Choi, S. Park, S. Yoon, N. Stubbs, Nondestructive damage identification in plate structures using changes in modal compliance, *NDT & E International* 38 (7) (2005) 529–540.
- [20] A.C. Ugural, *Stresses in Plates and Shells*, McGraw-Hill, New York, 1981.
- [21] S. Park, Development of a methodology to continuously monitor the safety of complex structures. Ph.D. Dissertation, Texas A&M University, 1997.
- [22] S. Choi, S. Park, N. Stubbs, Nondestructive damage detection in structures using changes in compliance, *International Journal of Solids and Structures* 42 (2005) 4494–4513.
- [23] J.D. Gibson, J.L. Melsa, *Introduction to Nonparametric Detection with Applications*, Academic Press, New York, 1975.
- [24] ABAQUS, Version 6.2 User's Manual, Hibbitt, Karlsson & Sorensen Inc., Providence, RI, 2001.
- [25] J.T. Kim, N. Stubbs, Model-uncertainty impact and damage-detection accuracy in plate girder, *ASCE Journal of Structural Engineering* 121 (10) (1994) 1409–1417.